Chemoattractants and chemorepellents act by inducing opposite polarity in phospholipase C and PI3-kinase signaling

Ineke Keizer-Gunnink, Arjan Kortholt, and Peter J.M. Van Haastert

Department of Molecular Cell Biology, University of Groningen, 9751NN Haren, Netherlands

During embryonic development, cell movement is orchestrated by a multitude of attractants and repellents. Chemoattractants applied as a gradient, such as cAMP with *Dictyostelium discoideum* or fMLP with neutrophils, induce the activation of phospholipase C (PLC) and phosphoinositide 3 (PI3)-kinase at the front of the cell, leading to the localized depletion of phosphatidylinositol 4,5-bisphosphate (PI[4,5]P_2) and the accumulation of phosphatidylinositol-3,4,5-trisphosphate (PI[3,4,5]P_3). Using *D. discoideum*, we show that chemorepellent cAMP analogues induce localized inhibition of PLC, thereby reversing the polarity of PI(4,5)P_2. This leads to the accumulation of PI(3,4,5)P_3 at the rear of the cell, and chemotaxis occurs away from the source. We conclude that a PLC polarity switch controls the response to attractants and repellents.

Introduction

Chemotaxis is a pivotal response of many cells to spatial cues (Van Haastert and Devreotes, 2004; Affolter and Weijer, 2005; Wu, 2005). It plays important roles in diverse functions, such as finding nutrients in prokaryotes, forming multicellular structures in protozoa, and tracking bacterial infections in neutrophils (Baggiolini, 1998; Campbell and Butcher, 2000; Crone and Lee, 2002). Research on directional movement by external cues in eukaryotes is dominated by chemoattraction, which is the movement toward the chemical compound. Repellents play an important role in morphogenesis, especially during embryonic development (Yang et al., 2002; Schmitt et al., 2005). Cell movement during chick primitive streak formation is controlled by FGF8-mediated chemorepulsion of the cells away from the streak, followed by chemoattraction toward the FGF4 signal produced by the forming notochord (Yang et al., 2002). Axon guidance during spinal chord development away from the roof plate is regulated by multiple repellents, such as BMP (Butler and Dodd, 2003), and by the attractant netrin toward the floor plate (Kennedy et al., 2006).

The mechanism by which repellents work is not well known (Dormann and Weijer, 2006). We envision that a critical step of the signal transduction pathway for cell movement is stimulated by a chemoattractant and inhibited by a repellent. It is essential that this hypothetical step is somehow connected with cell polarity to obtain directional movement. *Dictyostelium discoideum* cells have been instrumental in resolving the mechanism by which cells sense and respond to chemoattractants. It has been shown that phosphatidylinositol-3,4,5-trisphosphate (PI[3,4,5]P_3), which is formed at the side of the cell closest to the source of chemoattractant, is a very strong inducer of pseudopod extensions (Parent et al., 1998; Hirsch et al., 2000; Servant et al., 2000; Funamoto et al., 2002; Iijima and Devreotes, 2002). *D. discoideum* cells are known to be repelled by unidentified compounds that are secreted by starving cells (Keating and Bonner, 1977; Kakebeeke et al., 1979), indicating that *D. discoideum* cells have a mechanism to process repellents. Previously, we have shown that several analogues of the attractant cAMP behave as a repellent (Van Haastert et al., 1984). The analogues mediate their effect through binding to the surface cAMP receptor cAR1 (Johnson et al., 1992), and they can be polar (3′deoxy, 3′amino-cAMP; 3′NH-cAMP) or lipophilic (8-para-chlorphenylthio-cAMP; 8CPT-cAMP). The analogues induce many signaling responses that are essentially identical to the responses induced by cAMP, including activation and adaptation of adenylyl and guanylyl cyclase (Peters et al., 1991; Bominaar and Van Haastert, 1993, 1994). We show that these analogues inhibit PLC, contrary to activation of PLC by cAMP. As a consequence, they induce dominant PI(3,4,5)P_3 signaling in the rear of the cell, by which cells move away from the repellent.

Correspondence to P.J.M. van Haastert: P.J.M.van.Haastert@rug.nl

Abbreviations used in this paper: PI3K, phosphoinositide 3 kinase PI(3,4,5)P_3, phosphatidylinositol-3,4,5-trisphosphate; PI(4,5)P_2, phosphatidylinositol 4,5-bisphosphate.

The online version of this article contains supplemental material.

The Journal of Cell Biology, Vol. 177, No. 4, May 21, 2007 579–585
http://www.jcb.org/cgi/doi/10.1083/jcb.200611046

Results and discussion

D. discoideum cells were stimulated with a micropipette containing either the agonist cAMP or the commercially available antagonist 8CPT-cAMP. The cells moved toward the pipette with cAMP, but did not move effectively toward the pipette with 8CPT-cAMP, and actually moved away from the pipette (Fig. S1 and Videos 1 and 2, available at http://www.jcb.org/cgi/content/full/jcb.200611046/DC1). Experiments have been repeated with 3′NH-cAMP, yielding the same results as with 8CPT-cAMP (unpublished data). Fig. 1 A shows four frames from a movie in which cells were stimulated with two pipettes containing cAMP and 8CPT-cAMP, respectively (Video 3). In buffer, cells move in random directions (Fig. 1 A, 1 min), and cells move away from the pipette with 8CPT-cAMP (Fig. 1 A, 16 min). Upon application of the pipette with cAMP (cAMP and 8CPT-cAMP; Fig. 1 A, 26 min) cells moved in nearly random directions. However, upon withdrawal of the pipette containing 8CPT-cAMP, cells immediately moved toward the pipette with cAMP (Fig. 1 A, 38 min). The trajectories of the cells were analyzed. Data are presented as the chemotaxis index, which is the distance moved in the direction of the gradient ("upgradient") divided by the total distance moved in 30-s intervals. Data from Video 3 are presented in Fig. 1 B, and the means and the SEMs for six independent experiments are presented in Fig. 1 C. Wild-type cells show an excellent chemotactic response toward cAMP, with a chemotaxis index of 0.81 ± 0.05. Cells are not attracted to the pipette containing 8CPT-cAMP, but instead exhibit a significant negative chemotaxis index of -0.52 ± 0.04 ($P < 0.005$). The chemotaxis index of cells stimulated simultaneously with cAMP and 8CPT-cAMP is -0.18 ± 0.11, indicating that 8CPT-cAMP antagonizes the positive chemotaxis toward cAMP and cAMP antagonizes the negative chemotaxis induced by 8CPT-cAMP. Finally, starting with stimulation by the two pipettes, upon withdrawal of the pipette with 8CPT-cAMP the chemotaxis index toward cAMP rapidly increases to 0.72 ± 0.06. The results demonstrate that 8CPT-cAMP is a repellent that can reversibly inhibit the chemotactic response to cAMP.

D. discoideum cells move using actin filaments in the front of the cell, which induce the formation of local pseudopodia, and actomyosin filaments in the rear of the cell, which inhibit pseudopod formation and retract the uropod. We coexpressed Myosin-RFP and the filamentous actin-binding protein LimE-GFP from a single plasmid. A pipette with cAMP induces the expected movement of the cells upgradient with LimE-GFP localized in the front and Myosin-RFP in the rear of the cell (Fig. 2 A and Video 4, available at http://www.jcb.org/cgi/content/full/jcb.200611046/DC1). Interestingly, the localization of LimE-GFP in the protruding front and Myosin-RFP in the retracting back is identical in cells stimulated with 8CPT-cAMP, except that the front is downgradient and cells move away from the pipette (Fig. 2 A and Video 5).

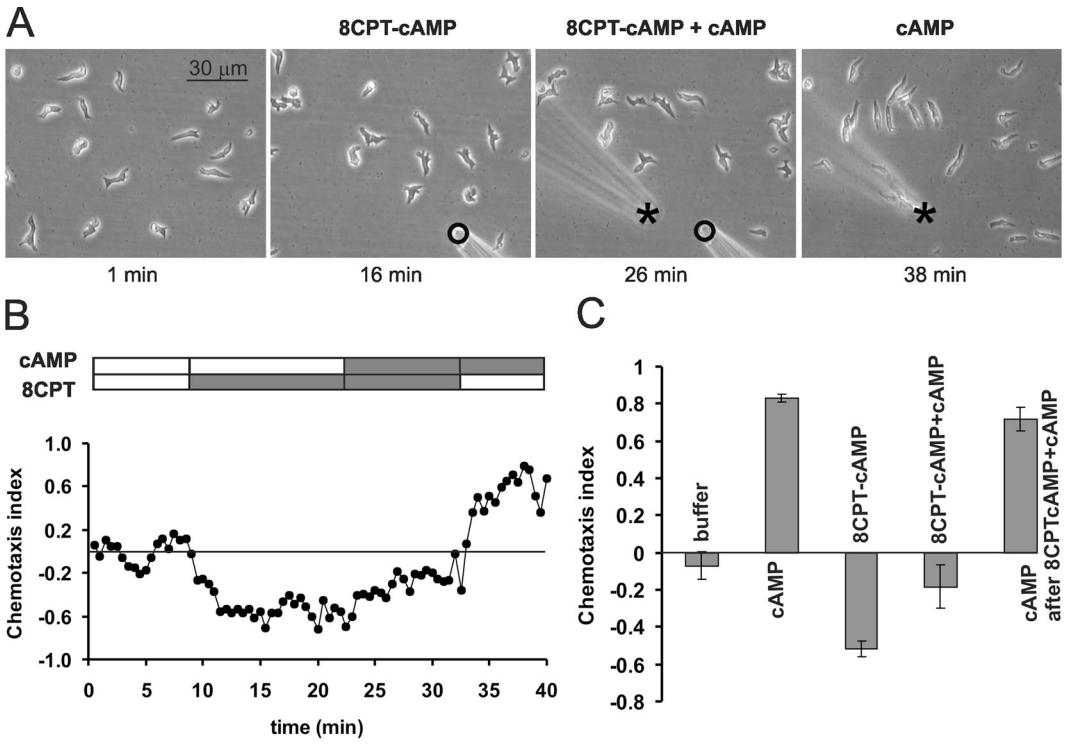

Figure 1. **Antagonism of chemotaxis to cAMP by 8CPT-cAMP.** Starved *D. discoideum* cells were spread on a polystyrene surface in a droplet with 0.5 ml of 10 mM phosphate buffer, pH 6.1, at room temperature, and stimulated by micropipettes filled with 10 mM 8CPT-cAMP (bottom right, open circle) or 0.1 mM cAMP (top left, asterisk); see Materials and methods for further details. (A) Four frames from a movie (Video 3) showing the distribution of cells without stimulus, 8 min after stimulation with 8CPT-cAMP, 5 min after stimulation with 8CPT-cAMP and cAMP, and 12 min after stimulation with cAMP alone (by removing the pipette with 8CPT-cAMP). (B) The chemotaxis index was determined for 20 cells that were shown in Video 3; (top) the filled sections show the simulation with cAMP and/or 8CPT-cAMP. (C) The chemotaxis index was calculated for 85 cells from 6 independent experiments; data shown are the mean ± the SEM. Video 3 is available at http://www.jcb.org/cgi/content/full/jcb.200611046/DC1.

To investigate the mechanism by which 8CPT-cAMP induces negative chemotaxis, wild-type cells expressing the $PI(3,4,5)P_3$ detector PHcracGFP were stimulated with cAMP and 8CPT-cAMP. Similar to previous investigations (Parent et al., 1998; Huang et al., 2003), a pipette with cAMP induces strong localization of PHcracGFP to the plasma membrane at the upgradient side of the cell. Pseudopodia are extended from PHcracGFP-containing areas and cells move upgradient toward the pipette (Fig. 2 B and Video 6, available at http://www.jcb.org/cgi/content/full/jcb.200611046/DC1). 8CPT-cAMP also induces strong localization of PHcracGFP at the plasma membrane, but with opposite polarity compared with cAMP, which is downgradient (Fig. 2 B and Video 7). Cells extend pseudopodia from these PHcracGFP-containing areas, and therefore move away from the pipette with 8CPT-cAMP. The size of the PHcracGFP patches induced by 8CPT-cAMP (9.0 ± 0.43 μm) is only slightly larger than the patches induced by cAMP (6.6 ± 0.17 μm), indicating that 8CPT-cAMP effectively reverses the $PI(3,4,5)P_3$ polarity.

$PI(3,4,5)P_3$ is formed by PI3-kinase (PI3K) and degraded by PTEN that, in cAMP gradients, are localized at the leading edge and the rear of the cell, respectively. In 8CPT-cAMP gradients, the localization of PI3K and PTEN is reversed compared with cAMP gradients (Fig. 2 B). To investigate the role of PI3K activity in polarity and chemotaxis reversal, we investigated the chemotactic activity of *pi3k1/2*$^-$-null cells toward cAMP and 8CPT-cAMP. In *pi3k1/2*$^-$-null cells, two PI3Ks are deleted that, together, mediate the vast majority of cAMP-stimulated $PI(3,4,5)P_3$ production (Zhou et al., 1998; Funamoto et al., 2002; Huang et al., 2003). These experiments are possible because PI3K is not essential for chemotaxis, and directional sensing can be mediated by other pathways (Hirsch et al., 2000;

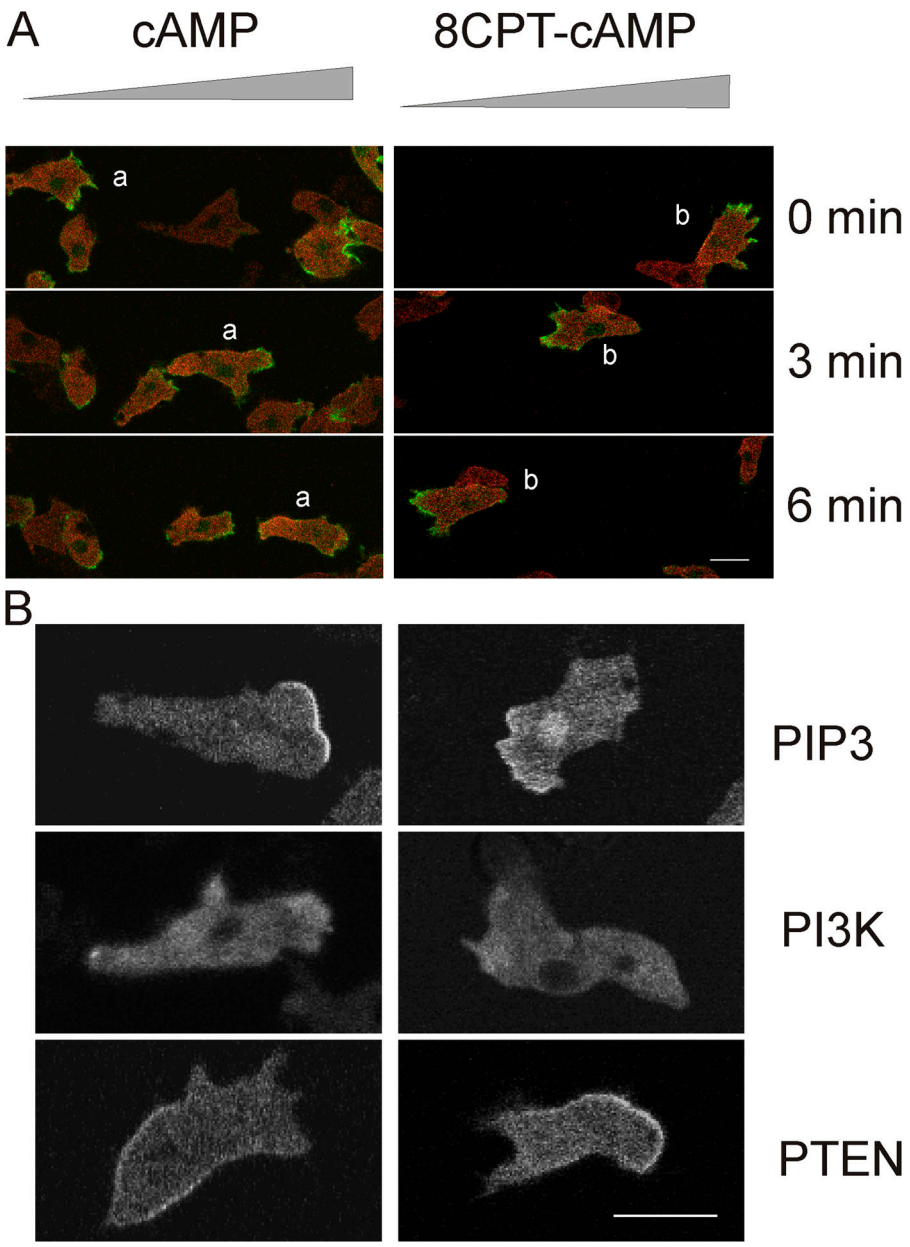

Figure 2. **Confocal fluorescent images of cells stimulated with cAMP or 8CPT-cAMP.** (A) Cells expressing myosin II-RFP (red) and the F-actin–binding protein LimE-GFP (green) were stimulated with cAMP or 8CPT-cAMP by pipettes that are positioned at the right. The figure shows 3 frames of a movie with 5-min intervals (cAMP, Video 4; 8CPT-cAMP, Video 5). (B) Cells expressing the $PI(3,4,5)P_3$ detector PHcrac-GFP, PI3K-GFP, or PTEN-GFP were stimulated with cAMP or 8CPT-cAMP by pipettes that are positioned at the right. The figure shows a representative cell for each case (a field of cells expressing PHcrac-GFP is presented in Video 4 for cAMP and Videos 5 and 6 for 8CPT-cAMP). Videos 4–6 are available at http://www.jcb.org/cgi/content/full/jcb.200611046/DC1.

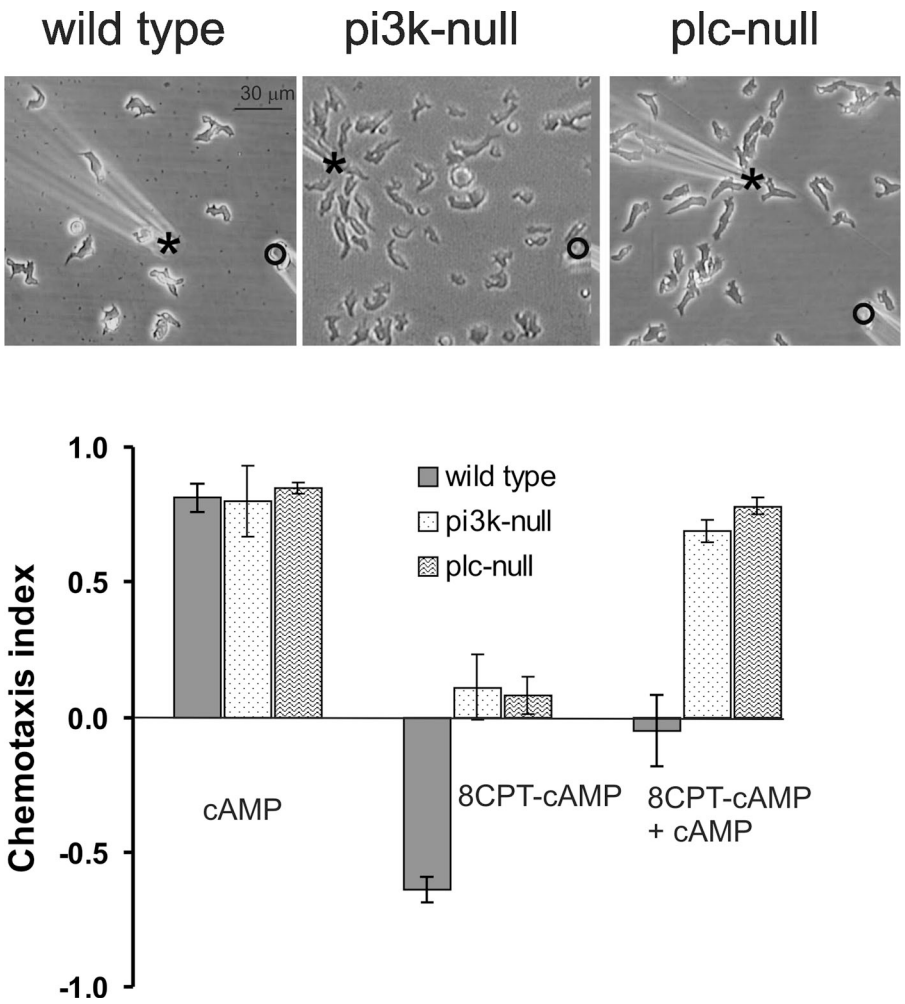

Figure 3. **Chemotaxis of mutants with deletions of PI3K or PLC.** (A) Frames from movies presenting the distribution of cells at 15 min after stimulation with both 8CPT-cAMP (open circles) and cAMP (asterisks) taken from Video 3 for WT cells, Video 8 for *pi3k1/2*-null cells, and Video 9 for *plc*-null cells. Wild-type cells show random distribution, whereas *pi3k1/2*-null and *plc*-null cells are attracted toward the pipette with cAMP. (B) Chemotaxis index of wild-type, *pi3k1/2*-null, and *plc*-null cells toward cAMP, 8CPT-cAMP, or 8CPT-cAMP and cAMP. The results show that wild-type cells move away from 8CPT-cAMP, whereas *pi3k1/2*-null and *plc*-null are not repelled from 8CPT-cAMP. Moreover, chemotaxis toward cAMP is antagonized by 8CPT-cAMP in wild-type cells, but not in *pi3k1/2*-null and *plc*-null cells. Videos 3, 8, and 9 are available at http://www.jcb.org/cgi/content/full/jcb.200611046/DC1.

Funamoto et al., 2002; Iijima and Devreotes, 2002; Huang et al., 2003; Postma et al., 2004; Loovers et al., 2006). Fig. 3 shows that *pi3k1/2*$^{-}$-null cells exhibit a good chemotactic response toward a pipette with cAMP (chemotaxis index is 0.80 ± 0.13). In contrast to the negative chemotaxis induced by 8CPT-cAMP in wild-type cells, *pi3k1/2*$^{-}$ null cells do not exhibit a significant negative or positive response to 8CPT-cAMP (chemotaxis index is 0.11 ± 0.12). More importantly, using two pipettes with cAMP and 8CPT-cAMP, respectively, *pi3k1/2*$^{-}$-null cells effectively move toward cAMP and are not inhibited by 8CPT-cAMP (Fig. 3 and Video 8, available at http://www.jcb.org/cgi/content/full/jcb.200611046/DC1), indicating that PI3K is essential for the repellent activity of 8CPT-cAMP and for the inhibitory effect of 8CPT-cAMP on cAMP chemoattraction.

The molecular mechanism by which cAMP mediates $PI(3,4,5)P_3$ accumulation upgradient in *D. discoideum* cells has been well described. PI3K is activated and enriched upgradient in the cell, whereas the $PI(3,4,5)P_3$-degrading enzyme PTEN strongly localizes downgradient in the cell (Funamoto et al., 2002; Iijima and Devreotes, 2002). PTEN has been demonstrated to bind to phosphatidylinositol-3,4,5-trisphosphate ($PI[4,5]P_2$), suggesting that $PI(4,5)P_2$ is depleted upgradient in the cell (Iijima et al., 2004). This depletion of $PI(4,5)P_2$ could be induced by several nonexclusive methods, such as the observed conversion of $PI(4,5)P_2$ to $PI(3,4,5)P_3$ upgradient by PI3K (Funamoto et al., 2002; Huang et al., 2003), but also by the conversion of $PI(4,5)P_2$ to $Ins(1,4,5)P_3$ and DAG by PLC, which is known to be activated by cAMP (Drayer and van Haastert, 1992; Bominaar et al., 1994). We propose a mechanism by which 8CPT-cAMP could revert the polarity of chemotactic sensing that is based on the observation that cAMP stimulates PLC, whereas 8CPT-cAMP inhibits this enzyme (Peters et al., 1991; Bominaar and Van Haastert, 1993; Bominaar and Van Haastert, 1994; supporting biochemical data are presented in Fig. S2, available at http://www.jcb.org/cgi/content/full/jcb.200611046/DC1). Upgradient stimulation of PLC by cAMP will lead to local depletion of $PI(4,5)P_2$, and thereby prevent PTEN binding, by which the upgradient $PI(3,4,5)P_3$ accumulation is stabilized. In contrast, the upgradient inhibition of PLC by 8CPT-cAMP will lead to the local accumulation of $PI(4,5)P_2$, thereby inducing PTEN binding and upgradient $PI(3,4,5)P_3$ degradation (Fig. 4). This relatively simple model for polarity reversal predicts that 8CPT-cAMP does not induce polarity switching in *plc*-null cells. *D. discoideum* cells contain a single *plc* gene encoding a PLCδ isoform (Drayer and van Haastert, 1992), which, like PI3K, is instrumental but not essential for chemotaxis (Drayer et al., 1994). Expression of GFP-tagged reporter proteins in *plc*-null cells reveal, as predicted, cytosolic

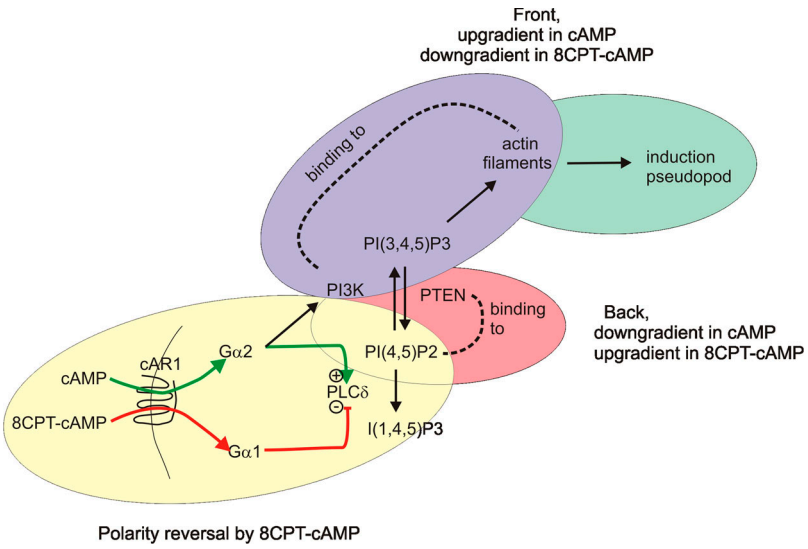

Figure 4. **Model for polarity reversal leading to cAMP-induced attraction and 8CPT-cAMP–induced repulsion.** The model contains three regulatory loops: first, a PLC activation/inhibition loop providing primary polarity of the $PI(4,5)P_2$ gradient; second, a $PI(4,5)P_2$/PTEN loop providing degradation of $PI(3,4,5)P_3$; and third, a PI3K/F-actin loop providing $PI(3,4,5)P_3$-mediated pseudopod extension. Because of inhibition of PLC by 8CPT-cAMP compared with stimulation by cAMP, the $PI(4,5)P_2$ polarity inverses, $PI(3,4,5)P_3$ accumulates downgradient, and cells move away from the pipette. The scheme is based on the observation that the $PI(3,4,5)P_3$-degrading enzyme PTEN binds to $PI(4,5)P_2$, whereas PI3K binds to actin filaments in the leading edge (Iijima et al., 2004; Sasaki et al., 2004), and on the observation that cAMP activates PLC, whereas 8CPT-cAMP inhibits this enzyme (Bominaar and Van Haastert, 1993, 1994; Peters et al., 1991). The mediating G proteins have been identified using knock-out cells (see supporting biochemical data in Fig. S1). Fig. S1 is available at http://www.jcb.org/cgi/content/full/jcb.200611046/DC1.

localization of PH-cracGFP and enhanced PTEN-GFP expression at the membrane in cAMP and 8CPT-cAMP gradients (Fig. S3). As presented in Fig. 3 B and Video 9, *plc*-null cells show a similar chemotactic response toward 8CPT-cAMP as *pi3k*-null cells: they move in random directions in the presence of 8CPT-cAMP alone and, subsequently, move effectively toward an additional pipette with cAMP. This indicates that PLC is also essential for mediating the inhibitory effect of 8CPT-cAMP, as is PI3K. Finally, *pten*-null cells were investigated, showing that these cells are attracted toward cAMP, but are not repelled by 8CPT-cAMP (unpublished data).

A scheme for $PI(3,4,5)P_3$-mediated chemotaxis reversal by 8CPT-cAMP consists of three parts (Fig. 4). The basis is a PLC/$PI(4,5)P_2$ polarity switch. In *D. discoideum*, PLC is regulated by the activating Gα2 and inhibitory Gα1, which, in a gradient of attractant or repellent, will determine the polarity of the $PI(4,5)P_2$ gradient. The attractant cAMP shows predominant activation of PLC, leading to lower $PI(4,5)P_2$ levels upgradient, while the repellent 8CPT-cAMP inhibits PLC, leading to higher $PI(4,5)P_2$ levels upgradient. The resulting gradients of $PI(4,5)P_2$ and colocalized PTEN mediate opposite gradients of $PI(3,4,5)P_3$, leading to the localized polymerization of actin. The gradients of localized PTEN and PI3K are stabilized because PTEN accumulates at the site of its product $PI(4,5)P_2$, whereas PI3K accumulates at sites of its effector, $PI(3,4,5)P_3$-induced F-actin. This mutually spatial exclusion of PI3K and PTEN will result in symmetry breaking, by which small spatial differences in the underlying polarity gradient can be amplified to the observed strong $PI(3,4,5)P_3$ gradient. Although PI3K and PLC are not essential for chemotaxis, the results clearly demonstrate that local formation of $PI(3,4,5)P_3$ is a very strong inducer of pseudopod formation, such that the cells can even move downgradient, overruling any upgradient signaling that 8CPT-cAMP may induce.

In our model, a compound is a repellent because it binds to a receptor that is preferentially coupled to PLC via an inhibitory G protein, whereas it is an attractant when the receptor is coupled to a stimulatory G protein. The regulation of *D. discoideum* PLC by the stimulatory G2 and inhibitory G1 forms the basis for the polarity switch, and it allows the cell to respond to chemical gradient with repulsion or attraction. This polarity switch may be used by the cell during development. *D. discoideum* cells grow on bacteria. Cells starved for <1 h secrete unidentified compounds that induce repulsion of the cells, by which cells may find bacteria in a larger area (Keating and Bonner, 1977; Kakebeeke et al., 1979). Cells starved for ∼5 h secrete cAMP, to which they are attracted and which allows the cells to form a multicellular structure. Interestingly, G1 is expressed throughout development, whereas G2 is nearly absent during early starvation and expressed only after ∼4 h (Pupillo et al., 1989). Thus, in early starved cells with the predominant inhibitory G1, the PLC–PI3K system is pruned for repulsion, whereas it becomes a system for attraction by expression of the stimulatory G2 during late starvation.

The mechanism of polarity reversal of PLC–PI3K signaling could be instrumental in mammalian cells to navigate in complex chemotactic gradients. During development, many cells, such as neurons and gonads, are projected in the body by mixtures of attractants and repellents (Yang et al., 2002; Schmitt et al., 2005). Observations on the action of Slit2 may be instrumental. Slit2 is a repellent for neuronal cells (Niclou et al., 2000; Ringstedt et al., 2000). In contrast, Slit2 does not affect the direction of movement of vascular smooth muscle cells, but strongly inhibits PDGF-stimulated chemotaxis by inhibition of PDGF stimulation of Rac1 (Wu et al., 2001; Chen et al., 2004). It is possible that, in neuronal cells, Slit2 induces a polar inhibition of Rac1, thereby inducing repulsion, whereas in vascular smooth muscle cells Slit2 induces uniform inhibition of Rac1 and is therefore not a repellent, but only an inhibitor of chemoattractants. Rac1 is known to be regulated by PIP3 in mammalian (Srinivasan et al., 2003; Kunisaki et al., 2006) and *D. discoideum* (Park et al., 2004) cells. The observed simplicity by which PLC-mediated polarity inversion of PI3K signaling in *D. discoideum* converts attraction to repulsion may provide a single mechanism to integrate complex positive and negative chemotactic signals during development.

Materials and methods

Plasmids and cells

The plasmid pWF38 (PHcracGFP) expressing the 700-bp N-terminal PH domain of CRAC fused to GFP (Parent et al., 1998), and plasmids expressing PI3K2-GFP (Funamoto et al., 2002; Iijima and Devreotes, 2002) and PTEN-GFP (Iijima and Devreotes, 2002) were provided by P. Devreotes (Johns Hopkins University School of Medicine, Baltimore, MD). Plasmid 339-3 expressing mRFPmars (Fischer et al., 2004) was provided by A. Muller-Taubenberger (Ludwig Maximilians University Munich, Munich, Germany). Plasmid pBIG-GFP-myo expressing a GFP fusion with myosin heavy chain II (Levi et al., 2002) was a gift from T. Egelhoff (Case Western Reserve University, Cleveland, OH). *pi3k1/2*-null cells were provided by R. Firtel (University of California, San Diego, La Jolla, CA).

Plasmid LB15B expressing LimE-GFP and Myo-RFP was constructed as follows. The neomycin resistance gene of MB74 was exchanged for the HPH hygromycin resistance gene that was preceded by an actin 15 promotor and terminated with a cabA terminator. The DNA coding for the actin-binding domain of LimE (aa 1–145) was cloned behind an actin 15 promoter and 5 adenosines, which serve as the Kozak sequence. It was followed by a SpeI site (coding for Thr and Ser) and the complete open reading frame of GFP (S65T variant), followed by a stop codon and an actin 8 terminator. This yielded the plasmid MB74hyg-LimE-GFP. The gene encoding the monomeric red fluorescent protein mRFPmars (Fischer et al., 2004) was amplified by PCR on plasmid DNA. The gene was preceded by a NgoMIV site, an actin 15 promotor, and 5 adenosines, and was followed by a BamHI site (encoding Gly and Ser), the sequence encoding aa 2–2116 of myosin heavy chain, the myosin terminator from the vector pBIG-GFP-myo (Levi et al., 2002), and a NgoMIV site. Finally, the gene encoding the mRFPmars-myosin fusion was released using the NgoMIV site and cloned into the single NgoMIV site of MB74hyg-LimE-GFP.

The *D. discoideum* strain AX3 was used as wild-type control in all experiments. The mutants strains used are the *plc*-null strain 1.19 (Drayer et al., 1995), the *pi3k*-null *pi3k1*$^-$/*pi3k2*$^-$ strain GMP1 (Funamoto et al., 2001), and *pten*-null cells (Iijima and Devreotes, 2002). Cells were grown in shaking culture in HG5 medium (containing per liter: 14.3 g oxoid peptone, 7.15 g bacto yeast extract, 1.36 g $Na_2HPO_4\times 12H_2O$, 0.49 g KH_2PO_4, 10.0 g glucose) at a density between 5×10^5 and 6×10^6 cells/ml. Cells were harvested by centrifugation for 3 min at 300 g, washed in PB (10 mM KH_2PO_4/Na_2HPO_4, pH 6.5), and starved in PB in 6-well plates (Nunc) for 5h. Cells were then resuspended in PB, centrifuged, and washed once in PB, and resuspended in PB at a density of 6×10^6 cells/ml.

Recording of movies

Unless otherwise mentioned, digital images of cells in PB at room temperature were captured at 10-s time intervals over 45 min. Videos 1, 2, 4, and 5–7 were captured using a confocal laser scanning microscope (LSM 510 META-NLO; Carl Zeiss Microimaging, Inc.) equipped with a 63×/NA 1.4 objective (Plan-Apochromatic; Carl Zeiss Microimaging, Inc.). For excitation of the fluorochromes, GFP (S65T variant), and mRFPmars, a 488-nm argon/krypton laser and a 543-nm helium laser were used, respectively. The fluorescence was filtered through a BP500-530 IR and a LP560 filter, and was detected by a photomultiplier tube. The field of observation is 206×206 μm; Videos 1 and 2 present the phase-contrast channel, whereas the fluorescent channel is shown in Videos 4–7. For Videos 3 and 9, an inverted light microscope (Type CK40 with a LWD A240 20×/NA 0.4 objective; Olympus) fitted with a charge-coupled device camera (TK-C1381; JVC) was used. Digital images were captured on a PC using VirtualDub software and Indeo video 5.10 compression. The field of observation is 358×269 μm. Video 8 was captured using a 10× numerical aperture 0.25 objective, and presents a selected field of the same size, namely 358×269 μm. For all individual videos, specific time periods were selected that start at the moment the pipette was lowered to the plane just above the cells. In the phase-contrast videos, the pipette tips are visible as dark triangular shadows. In the fluorescence videos (Videos 4–7), the place of the pipette tip is indicated with an asterisk.

Analysis of chemotaxis

The chemotaxis index, which is defined as the ratio of the cell displacement in the direction of the gradient and its total traveled distance, was determined for ~25 cells in a video, as follows. First, the position of the centroid of a cell was determined with ImageJ (National Institutes of Health; rsb.info.nih.gov/ij) for frames at 30-s intervals, yielding a series of coordinates for that cell. Using these coordinates, the chemotaxis index of each 30-s step was calculated and averaged, yielding the chemotaxis index for that cell in the movie. The data shown are the average and SEM of the chemotaxis indices from at least three independent experiments, with ~25 cells per experiment.

Online supplemental material

Fig. S1 shows cell trajectories of wild-type cells in a gradient of cAMP and 8CPT-cAMP, revealing that cells are attracted toward cAMP, but repelled from 8CPT-cAMP. Fig. S2 shows inhibition of PLC signaling by the antagonist 3′NH-cAMP. 8CPT-cAMP has similar properties to 3′NH-cAMP. Fig. S3 shows the localization of PHcrac-GFP, PTEN-GFP, and PI3K-GFP in *plc*-null cells in a gradient of cAMP or 8CPT-cAMP. Video 1 shows chemotaxis toward a pipette with cAMP. Video 2 shows chemotaxis away from a pipette with 8CPT-cAMP. Video 3 shows cell movement in gradients of 8CPT-cAMP and cAMP+8CPT-cAMP, followed by movement in only cAMP. Video 4 shows the localization of F-actin at the leading edge and myosin in the back of cells chemotaxing toward cAMP. Video 5 shows the localization of F-actin at the leading edge and myosin in the back of cells chemotaxing away from 8CPT-cAMP. Video 6 shows the localization of PHcracGFP (detecting $PI[3,4,5]P_3$) at the leading edge of cells chemotaxing toward cAMP. Video 7 shows the localization of PHcracGFP (detecting $PI[3,4,5]P_3$) at the leading edge of cells chemotaxing away from 8CPT-cAMP. Video 8 shows chemotaxis of *pi3k1/2*-null cells toward cAMP in the presence of 8CPT-cAMP. Video 9 shows chemotaxis of *plc*-null cells toward cAMP in the presence of 8CPT-cAMP. The online version of this article is available at http://www.jcb.org/cgi/content/full/jcb.200611046/DC1.

We thank B. Jastorff for a kind gift of 3′NH-cAMP; A. Bominaar for data on PLC regulation by 3′NH-cAMP; R. Firtel for *pi3k1/2*-null cells; P. Devreotes for plasmids expressing PHcracGFP, PI3K2-GFP, and PTEN-GFP; A. Muller-Taubenberger for plasmid expressing mRFPmars; T. Egelhoff for plasmid expressing a GFP fusion with myosin heavy chain II; and Dr. L Bosgraaf for plasmid expressing LimE-GFP/Myo-RFP. Plasmids and cells were obtained through the *Dictyostelium* Stock Center.

Submitted: 9 November 2006
Accepted: 18 April 2007

References

Affolter, M., and C.J. Weijer. 2005. Signaling to cytoskeletal dynamics during chemotaxis. *Dev. Cell*. 9:19–34.

Baggiolini, M. 1998. Chemokines and leukocyte traffic. *Nature*. 392:565–568.

Bominaar, A.A., F. Kesbeke, and P.J.M. Van Haastert. 1994. Phospholipase C in *Dictyostelium discoideum*. Cyclic AMP surface receptor and G-protein-regulated activity in vitro. *Biochem. J.* 297:181–187.

Bominaar, A.A., and P.J.M. Van Haastert. 1993. Chemotactic antagonists of cAMP inhibit *Dictyostelium* phospholipase C. *J. Cell Sci.* 104:181–185.

Bominaar, A.A., and P.J.M. Van Haastert. 1994. Phospholipase C in *Dictyostelium discoideum*. Identification of stimulatory and inhibitory surface receptors and G-proteins. *Biochem. J.* 297:189–193.

Butler, S.J., and J. Dodd. 2003. A role for BMP heterodimers in roof plate-mediated repulsion of commissural axons. *Neuron*. 38:389–401.

Campbell, J.J., and E.C. Butcher. 2000. Chemokines in tissue-specific and microenvironment-specific lymphocyte homing. *Curr. Opin. Immunol.* 12:336–341.

Chen, B., D.G. Blair, S. Plisov, G. Vasiliev, A.O. Perantoni, Q. Chen, M. Athanasiou, J.Y. Wu, J.J. Oppenheim, and D. Yang. 2004. Cutting edge: bone morphogenetic protein antagonists Drm/Gremlin and Dan interact with Slits and act as negative regulators of monocyte chemotaxis. *J. Immunol.* 173:5914–5917.

Crone, S.A., and K.F. Lee. 2002. The bound leading the bound: target-derived receptors act as guidance cues. *Neuron*. 36:333–335.

Dormann, D., and C.J. Weijer. 2006. Chemotactic cell movement during *Dictyostelium* development and gastrulation. *Curr. Opin. Genet. Dev.* 16:367–373.

Drayer, A.L., and P.J.M. van Haastert. 1992. Molecular cloning and expression of a phosphoinositide-specific phospholipase C of *Dictyostelium* discoideum. *J. Biol. Chem.* 267:18387–18392.

Drayer, A.L., J. van der Kaay, G.W. Mayr, and P.J.M. van Haastert. 1994. Role of phospholipase C in *Dictyostelium*: formation of inositol 1,4,5-trisphosphate and normal development in cells lacking phospholipase C activity. *EMBO J.* 13:1601–1609.

Drayer, A.L., M.E. Meima, M.W.M. Derks, R. Tuik, and P.J.M. van Haastert. 1995. Mutation of an EF-hand Ca2+-binding motif in phospholipase

C of *Dictyostelium* discoideum: inhibition of activity but no effect on Ca2+-dependence. *Biochem. J.* 311:505–510.

Fischer, M., I. Haase, E. Simmeth, G. Gerisch, and A. Muller-Taubenberger. 2004. A brilliant monomer red fluorescent protein to visualize cytoskeleton dynamics in *Dictyostelium*. *FEBS Lett.* 577:227–232.

Funamoto, S., K. Milan, R. Meili, and R.A. Firtel. 2001. Role of phosphatidylinositol 3′ kinase and a downstream pleckstrin homology domain–containing protein in controlling chemotaxis in *Dictyostelium*. *J. Cell Biol.* 153:795–809.

Funamoto, S., R. Meili, S. Lee, L. Parry, and R.A. Firtel. 2002. Spatial and temporal regulation of 3-phosphoinositides by PI 3-kinase and PTEN mediates chemotaxis. *Cell*. 109:611–623.

Hirsch, E., V.L. Katanaev, C. Garlanda, O. Azzolino, L. Pirola, L. Silengo, S. Sozzani, A. Mantovani, F. Altruda, and M.P. Wymann. 2000. Central role for G protein-coupled phosphoinositide 3-kinase gamma in inflammation. *Science*. 287:1049–1053.

Huang, Y.E., M. Iijima, C.A. Parent, S. Funamoto, R.A. Firtel, and P.N. Devreotes. 2003. Receptor mediated regulation of PI3Ks confines PI(3,4,5)P3 to the leading edge of chemotaxing cells. *Mol. Biol. Cell*. 14:1913–1922.

Iijima, M., and P. Devreotes. 2002. Tumor suppressor PTEN mediates sensing of chemoattractant gradients. *Cell*. 109:599–610.

Iijima, M., Y.E. Huang, H.R. Luo, F. Vazquez, and P.N. Devreotes. 2004. Novel mechanism of PTEN regulation by its PIP2 binding motif is critical for chemotaxis. *J. Biol. Chem.* 279:16606–16613.

Johnson, R.L., P.J. Van Haastert, A.R. Kimmel, C.L. Saxe III, B. Jastorff, and P.N. Devreotes. 1992. The cyclic nucleotide specificity of three cAMP receptors in *Dictyostelium*. *J. Biol. Chem.* 267:4600–4607.

Kakebeeke, P.I., R.J. de Wit, S.D. Kohtz, and T.M. Konijn. 1979. Negative chemotaxis in *Dictyostelium* and *Polysphondylium*. *Exp. Cell Res.* 124:429–433.

Keating, M.T., and J.T. Bonner. 1977. Negative chemotaxis in cellular slime molds. *J. Bacteriol.* 130:144–147.

Kennedy, T.E., H. Wang, W. Marshall, and M. Tessier-Lavigne. 2006. Axon guidance by diffusible chemoattractants: a gradient of netrin protein in the developing spinal cord. *J. Neurosci.* 26:8866–8874.

Kunisaki, Y., A. Nishikimi, Y. Tanaka, R. Takii, M. Noda, A. Inayoshi, K. Watanabe, F. Sanematsu, T. Sasazuki, T. Sasaki, and Y. Fukui. 2006. DOCK2 is a Rac activator that regulates motility and polarity during neutrophil chemotaxis. *J. Cell Biol.* 174:647–652.

Levi, S., M.V. Polyakov, and T.T. Egelhoff. 2002. Myosin II dynamics in *Dictyostelium*: determinants for filament assembly and translocation to the cell cortex during chemoattractant responses. *Cell Motil. Cytoskeleton*. 53:177–188.

Loovers, H., M. Postma, I. Keizer-Gunnink, Y.E. Huang, P.N. Devreotes, and P.J.M. Van Haastert. 2006. Distinct roles of PI(3,4,5)P3 during chemoattractant signaling in *Dictyostelium*: A quantitative in vivo analysis by inhibition of PI3-kinase. *Mol. Biol. Cell*. 17:1503–1513.

Niclou, S.P., L. Jia, and J.A. Raper. 2000. Slit2 is a repellent for retinal ganglion cell axons. *J. Neurosci.* 20:4962–4974.

Parent, C.A., B.J. Blacklock, W.M. Froehlich, D.B. Murphy, and P.N. Devreotes. 1998. G protein signaling events are activated at the leading edge of chemotactic cells. *Cell*. 95:81–91.

Park, K.C., F. Rivero, R. Meili, S. Lee, F. Apone, and R.A. Firtel. 2004. Rac regulation of chemotaxis and morphogenesis in *Dictyostelium*. *EMBO J.* 23:4177–4189.

Peters, D.J., A.A. Bominaar, B.E. Snaar-Jagalska, R. Brandt, P.J. Van Haastert, A. Ceccarelli, J.G. Williams, and P. Schaap. 1991. Selective induction of gene expression and second-messenger accumulation in *Dictyostelium* discoideum by the partial chemotactic antagonist 8-p-chlorophenylthioadenosine 3′,5′-cyclic monophosphate. *Proc. Natl. Acad. Sci. USA*. 88:9219–9223.

Postma, M., J. Roelofs, J. Goedhart, H.M. Loovers, A.J.W.G. Visser, and P.J.M. Van Haastert. 2004. Sensitisation of *Dictyostelium* chemotaxis by PI3-kinase mediated self-organising signalling patches. *J. Cell Sci.* 117:2925–2935.

Pupillo, M., A. Kumagai, G.S. Pitt, R.A. Firtel, and P.N. Devreotes. 1989. Multiple alpha subunits of guanine nucleotide-binding proteins in *Dictyostelium*. *Proc. Natl. Acad. Sci. USA*. 86:4892–4896.

Ringstedt, T., J.E. Braisted, K. Brose, T. Kidd, C. Goodman, M. Tessier-Lavigne, and D.D. O'Leary. 2000. Slit inhibition of retinal axon growth and its role in retinal axon pathfinding and innervation patterns in the diencephalon. *J. Neurosci.* 20:4983–4991.

Sasaki, A.T., C. Chun, K. Takeda, and R.A. Firtel. 2004. Localized Ras signaling at the leading edge regulates PI3K, cell polarity, and directional cell movement. *J. Cell Biol.* 167:505–518.

Schmitt, A.M., J. Shi, A.M. Wolf, C.C. Lu, L.A. King, and Y. Zou. 2006. Wnt-Ryk signalling mediates medial-lateral retinotectal topographic mapping. *Nature*. 439:31–37.

Servant, G., O.D. Weiner, P. Herzmark, T. Balla, J.W. Sedat, and H.R. Bourne. 2000. Polarization of chemoattractant receptor signaling during neutrophil chemotaxis. *Science*. 287:1037–1040.

Srinivasan, S., F. Wang, S. Glavas, A. Ott, F. Hofmann, K. Aktories, D. Kalman, and H.R. Bourne. 2003. Rac and Cdc42 play distinct roles in regulating $PI(3,4,5)P_3$ and polarity during neutrophil chemotaxis. *J. Cell Biol.* 160:375–385.

Van Haastert, P.J.M., and P.N. Devreotes. 2004. Chemotaxis: signalling the way forward. *Nat. Rev. Mol. Cell Biol.* 5:626–634.

Van Haastert, P.J.M., R. Van Driel, B. Jastorff, J. Baraniak, W.J. Stec, and R.J. De Wit. 1984. Competitive cAMP antagonists for cAMP-receptor proteins. *J. Biol. Chem.* 259:10020–10024.

Wu, D. 2005. Signaling mechanisms for regulation of chemotaxis. *Cell Res.* 15:52–56.

Wu, J.Y., L. Feng, H.T. Park, N. Havlioglu, L. Wen, H. Tang, K.B. Bacon, Z. Jiang, X. Zhang, and Y. Rao. 2001. The neuronal repellent Slit inhibits leukocyte chemotaxis induced by chemotactic factors. *Nature*. 410:948–952.

Yang, X., D. Dormann, A.E. Munsterberg, and C.J. Weijer. 2002. Cell movement patterns during gastrulation in the chick are controlled by positive and negative chemotaxis mediated by FGF4 and FGF8. *Dev. Cell*. 3:425–437.

Zhou, K., S. Pandol, G. Bokoch, and A.E. Traynor-Kaplan. 1998. Disruption of *Dictyostelium* PI3K genes reduces [32P]phosphatidylinositol 3,4 bisphosphate and [32P]phosphatidylinositol trisphosphate levels, alters F-actin distribution and impairs pinocytosis. *J. Cell Sci.* 111:283–294.